Journal of Materials Chemistry B

Accepted Manuscript

This is an *Accepted Manuscript*, which has been through the Royal Society of Chemistry peer review process and has been accepted for publication.

Accepted Manuscripts are published online shortly after acceptance, before technical editing, formatting and proof reading. Using this free service, authors can make their results available to the community, in citable form, before we publish the edited article. We will replace this *Accepted Manuscript* with the edited and formatted *Advance Article* as soon as it is available.

You can find more information about *Accepted Manuscripts* in the Information for Authors.

Please note that technical editing may introduce minor changes to the text and/or graphics, which may alter content. The journal's standard Terms & Conditions and the Ethical guidelines still apply. In no event shall the Royal Society of Chemistry be held responsible for any errors or omissions in this *Accepted Manuscript* or any consequences arising from the use of any information it contains.

ROYAL SOCIETY OF CHEMISTRY

www.rsc.org/materialsB

Journal of Materials Chemistry B ARTICLE

Durable keratin based bilayered electrospun mats for wound closure †

*Received 00th January 20xx,
Accepted 00th January 20xx

DOI: 10.1039/x0xx00000x
www.rsc.org/

Sivakumar Singaravelu[a#], Giriprasath Ramanathan[a#], Thangavelu Muthukumar[b], M. D. Raja[a], Naveen Nagiah[c], Sitalakshmi Thyagarajan[a], Adithan Aravinthan[b], Gunasekaran. P[d], Natarajan. T. S[e], V. N. Geetha Selva Gangai[f], Jong-hoon Kim[*b], Uma Tiruchirapalli Sivagnanam[*a]

The bilayered nanofibrous scaffold with rapid wound healing properties will be found to be suitable for tissue regeneration application. The objective of this study is to reveal the fabrication of Poly (3-hydroxybutyric acid) (P) - Gelatin (G) nanofibrous mat with horn Keratin-Chitosan based biosheet (KC) as a bilayered nanofibrous scaffold through electrospinning. The Mupirocin (D) loaded horn KC biosheet (KCD) is act as the primary layer over which PG nanofiber were electrospun to act as the secondary layer. This engineered bilayered nanofibrous scaffold material (KC-PG) should fulfill the functions of extracellular matrix (ECM) by elucidating its function *in vitro* and *in vivo*. The bilayered nanofibrous scaffold were designed to exhibit improved physiochemical, biological, mechanical property with better swelling and porosity for enhanced oxygen permeability and it also acquires acceptable antibacterial property to prevent infection at the wound site. The bilayered nanofibrous scaffold assists in better biocompatibility against fibroblast and keratinocytes cell lines. The morphology of the nanofibrous scaffold aids to posses increased cell adhesion and proliferation with cell material interaction. This was elucidated with the help of *in vitro* fluorescence staining using against both cell lines. The bilayered KCD-PG nanofibrous scaffold materials possess accelerated wound healing efficiency during *in vivo* wound healing. The results influenced the regulation of growth factors with enhanced collagen synthesis, thereby helps in faster wound healing.

Introduction

The fundamental goal of skin tissue engineering is to develop an environmental friendly biomaterial to replace the damaged tissue using protein based nanofibrous material for wounds.[1] The skin wound debridement caused by accident or burn has turned the focus on the development of biomaterial for the affected people.[2] The healing of wounds is a complex process that involves in both biological and molecular integration of events such as cell adhesion, proliferation, ECM deposition, inflammation, angiogenesis and tissue remodeling.[3] The complex mechanism of wound healing involves in the cellular interaction with the immune and epidermal cells towards the fast healing. Growth factors play an important role in accelerating the healing with the presence of vascular endothelial growth factor (VEGF), [4] epidermal growth factor (EGF) [5] and transforming growth factor (TGF-β) [6]. VEGF is known to play a vital role in stimulating angiogenesis, cell signaling and prevalent in collagen deposition for proper healing. EGF enhances the epidermal growth, cell migration and proliferation essential for the tissue repair and regeneration in the early stage of wound healing.[7] TGF-β stimulates the growth factors secreted by both platelets and macrophages in cell differentiation for promoting rapid healing of the wounds.[8, 9]

Biomaterials based tissue engineering aims at achieving fabrication of robust biocompatible and biodegradable material with drug eluting properties that aid in enhanced wound healing/regeneration. The most important components of the ECM functions in the nanometer dimension of the cells were found to be highly dependent to serve as a suitable support site for cell adhesion and proliferation over the nanofiber matrix.[10] The nanofiber matrix provides high surface to volume ratio, good oxygen permeability and biocompatibility to impart cell adhesion to attain accelerated wound healing.[11] Accordingly, the support of biopolymers through nanofibrous scaffolds with the protein based biomimitic materials were desperately needed to regenerate the damaged tissues through bilayer nanofibrous scaffold approach as a wound dressing in wound healing application.[12]

Throughout the world, the bovine horn, a by-product of the slaughter house remains unutilized as a biowaste was recycled to keratin. Keratin (K), a fibrous structural protein with high cysteine residues

*a.Bioproducts Lab, CSIR-Central Leather Research Institute, Chennai-600020, Tamilnadu, India. *E-mail: suma67@gmail.com; Tel: + 91 44 24420709; Fax: +91 44 24911589*
b.Department of Physiology, College of Veterinary Medicine, Chonbuk National University, 79 Gobong-ro, Iksan-city, Jeollabuk-Do 570-752, Republic of Korea.
** E-mail: jhkim1@jbnu.ac.kr*
c.Department of Mechanical Engineering, University of Colorado, Boulder, USA.
d.Department of Virology, King Institute of Preventive Medicine and Research, Guindy, Chennai-600032, Tamilnadu, India.
e.Conducting Polymers Lab, Department of Physics, Indian Institute of Technology Madras, Chennai, India
f.Department of Biochemistry, Vikram Institute of Nursing and Paramedical Sciences, Mysore, Karnataka-570 002, India.
† Electronic Supplementary Information (ESI) available: Tabel and Figure.
 # Both have made equal contributions to this study

Journal of Materials Chemistry B Accepted Manuscript

Please do not adjust margins

has the active cell binding motifs to exhibits good cell material interaction towards accelerating wound healing property.[13] The keratin makes the scaffold more biocompatible and tends to have increased mechanical property due to the presence of disulfide bond.[14] Chitosan (C) is a favorable support material with hemostasis,[15] acceleration of tissue regeneration, migration of fibroblast and macrophages for efficient wound healing.[16] The hydrophobic polymer, poly (3-hydroxybutyric acid) (P), suits to have a functional support over the fibroblast and keratinocytes by exhibiting a biodegradablility[17] and mechanical property.[18] The P is non toxic since it is a common metabolite in all higher living organisms.[19] The major component of the ECM collagen, lose its property while electrospinning to form gelatin. However, the Gelatin (G) (denatured collagen) found to be suitable with its wide application in pharmaceutical field with excellent biocompatibility.[20] The antibacterial agent, mupirocin is often used topically at the wound site to prevent wound from infections. In addition, it is effective against both second degree and third degree burns.[21]

The dressing material has to possess all features towards the perfect biomaterial with good wound healing efficiency. However the use of a single polymer with all property will not facilitate in development of smart biomaterial. Moreover the blended system of both natural and synthetic polymers will aid to attain all ideal features to reach good healing proficiency.[22] In this perspective, the biopolymers blended to make keratin based biosheet to act as support material for the fabrication of novel bilayered nanofibrous matrix as a smart wound dressing material using a silicone splint model to make the healing process accurate, reproducible and minimizes wound contraction through granulation, reepithelialisation and to prove the maximum efficacy of prepared scaffold.[19] In addition, the property of single layered scaffold (biosheet and nanofibrous scaffold) were combined in the form of bilayered matrix to attain a maximum efficacy in wound closure and as a durable substitute in skin tissue engineering application.

The aim of the present work was to electrospun a nanofibrous mats from polymer blends of poly (3-hydroxybutyric acid) (P) and Gelatin (G) over the horn keratin based biosheet as a bilayered nanofibrous matrix scaffold as smart biomaterial for wound dressing application. The fabricated scaffolds were evaluated for their morphology, cell proliferation, mechanical property and expression levels of VEGF, EFG and TGF-β during the *in vivo* wound healing studies using silicone splint model using male albino Wistar rats.

Experimental Methods

Bovine horn was collected from the slaughter house at Perambur, Chennai, Tamil Nadu, India. Low-molecular-weight Chitosan (viscosity, 20–200 cps; 85 % acetylation), Poly(3-hydroxybutyric acid), Gelatin, 1,1,1,3,3,3 hexafluoro-2-propanol, 3-(4,5-dimethylthiazol-2-yl)-2,5-diphenyl tetrazolium bromide (MTT), 4,6-diamino-2-phenylindol (DAPI), Calcein AM, Dulbecco's modified Eagle's medium (DMEM), Fetal calf serum (FCS), and supplementary antibiotics for tissue culture were purchased from Sigma-Aldrich, India. The NIH 3T3 fibroblast and human (HaCaT) keratinocytes cell lines was obtained from the National Centre for Cell Science (NCCS), Pune, India. The rest of the chemicals were purchased from Sigma-Aldrich, unless specified otherwise. The sterilization of the bilayered nanofibrous matrix scaffolds was done by the ethylene oxide sterilization. All experiments were performed in compliance with Committee for the Purpose of Control and Supervision of Experiments on Animals guidelines (CPCSEA), and performed after the approval from the Institutional Animal Care and Use Committee (IACUC) [466/01a/CPCSEA].

Fabrication of semi solid KC biosheet

The bovine horn keratin (K) was extracted from the methods as reported from our previous work.[23] The fabrication of fully air dried KC biosheet was detailed in our previous work. In brief, K and 2 % (w/v) chitosan (C) solution were mixed in 1:3 ratio with 1.5 mL of ethylene glycol as a plasticizer to form the KC mixture. The prepared KC mixture was poured in polyethylene tray and fully air dried to obtain KC scaffold. However, semi solid KC biosheet was fabricated by pouring the prepared KC mixture into the polyethylene tray (measuring 16 cm X 18 cm) and air dried at room temperature until to get a semi solid KC biosheet (80 % dried). Similarly the KCD was prepared by incorporation of 50 mg of D. The prepared semi solid biosheet with the polyethylene tray was taken for electrospinning to fabricate a bilayered nanofibrous dual matrix scaffold.[23]

Electrospinning of bilayered nanofibrous matrix scaffold (KC-PG)

To prepare the KC-PG bilayered dual matrix, 4 % (w/v) concentration of polymer solution were prepared by dissolving 0.4 g of P and G in 10 mL of 1, 1, 1,3,3,3 hexafluoro-2-propanaol for 12h constant stirring. The blended solution of PG in 1:1 ratio was allowed at constant stirring for 8 h for uniform blending. The well blended solution were electrospuned over the prepared semi solid form of the KC biosheet placed over the grounded rectangle aluminum substrate at a distance of 13 cm perpendicular to the 24G needle connected to positive terminal of the high voltage DC power

Journal of Materials Chemistry B Accepted Manuscript

This journal is © The Royal Society of Chemistry 20xx

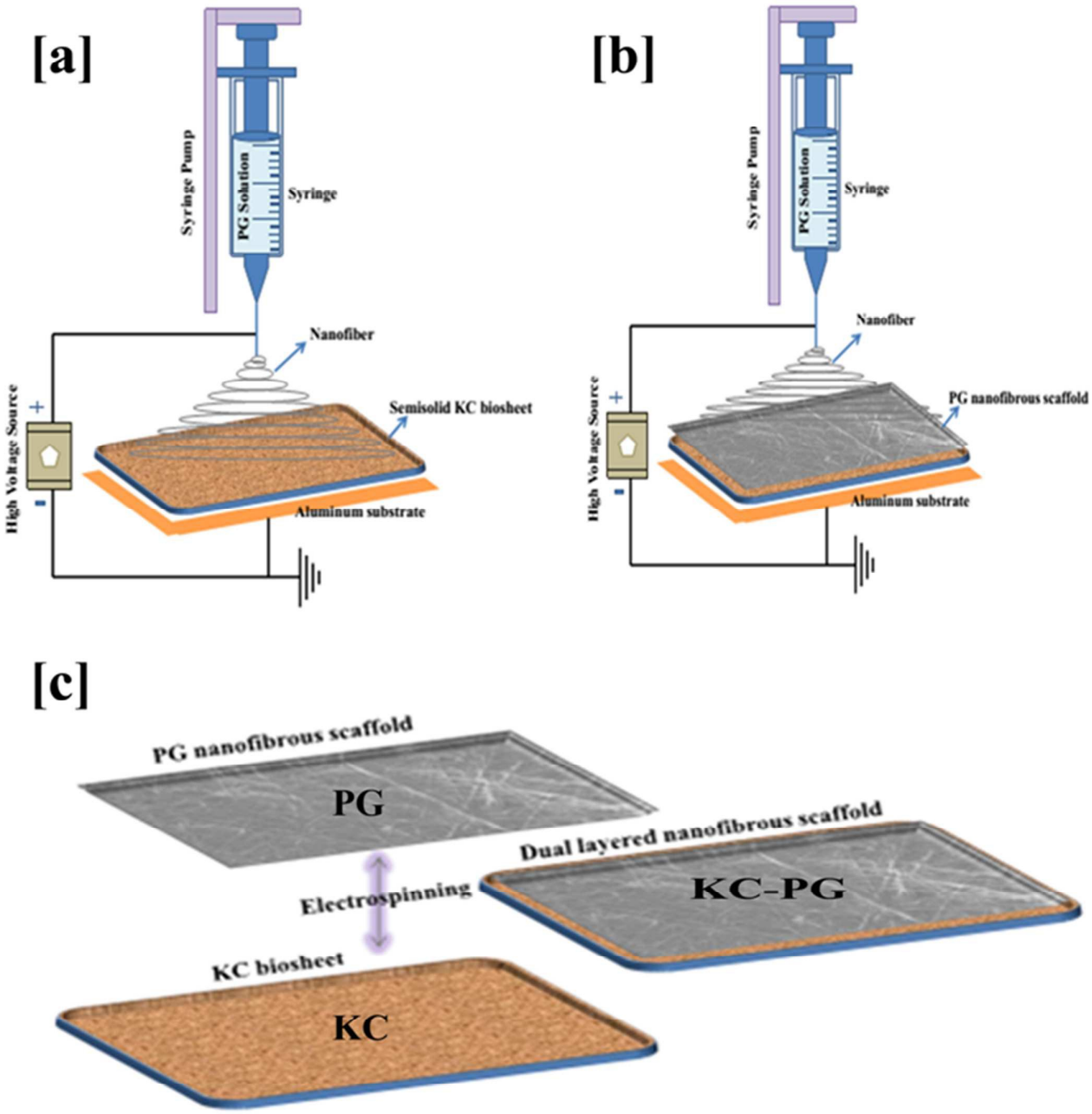

Scheme 1 Schematic illustration of fabrication of the bilayered nanofibrous KC-PG scaffold (a) PG deposited over the semisolid KC biosheet on a collecting plate via electrospinning process (b) Fabricated bilayered nanofibrous KC-PG scaffold (c) Simple representation of the bilayered nanofibrous matrix

supply (ZEONICS, Bangalore, India). The polymer solution was extruded with 1.5 mL/h using a controlled syringe pump subjected to an electric potential of 1.5 kV/cm. Therefore, after the evaporation of the solvent from the semisolid KC-PG scaffold, causing flatness PG nanofiber over the solidified KC biosheet to form the bilayered nanofibrous matrix (scheme1). Further the prepared scaffolds were stored at room temperature until further use.[24]

Characterization techniques

The chemical and conformational changes of the bilayered scaffold were investigated using Fourier transform infrared (FTIR) measurements, to determine the functional groups present in the prepared KC, PG, KC-PG and KCD-PG nanofibrous scaffolds were studied. The spectra were measured at a resolution of 4 cm^{-1} in the frequency range of 4000–600 cm^{-1} using ABB 3000 spectrometer with Grams as the operating software.[25] The surface morphology of

Journal of Materials Chemistry B Accepted Manuscript

Please do not adjust margins

the scaffolds were visualized using FE-SEM, (AURIGA, Carl Zeiss AG, Jena, Germany) operating at an accelerating voltage of 5– 20 kV after being coated with gold. Fifty different fibers were measured using the UTHSCSA Image tool software to determine the average diameter of the fibers for different concentrations of the polymer solution.[26] XPS spectra were obtained for the KC and KC-PG scaffolds in a SPECS XPS system (Germany) equipped with a twin anode X-ray source and a hemispherical analyzer with 150 W non-monochromatic Al Kα radiation (1486.6 eV). Core-level spectra of O1s, C1s, N1s and S1s were obtained at pass energy of 25 eV. The spectra were fitted with Gaussian peaks to find out the component peaks.[27]

Tensile strength measurement of the nanofibrous scaffolds

All the scaffolds were cut into dumb-bell shaped specimens (100x16 mm^2), prepared, and load-elongation measurement was measured using a universal testing machine (INSTRON model 1405) according to Vogel at an extension rate of 5 mm/min.[28]

Porosity

The porosity of the nanofibrous scaffold was determined *via* liquid displacement method using ethanol as the displacement liquid due to its easy penetration through the pores of the scaffolds which will not induce shrinking or swelling as a non solvent of the polymers.[26] A known weight (W) of the sample was immersed in a graduated cylinder containing a known volume (V_1) of ethanol. The samples were kept in ethanol for 5 min, and then a series of brief evacuation – repressurization cycles were conducted to force the ethanol in to the pores of the scaffold. The process was repeated until the air bubble stops. The total volume of the ethanol and the ethanol-impregnated scaffolds were then recorded as V_2. The difference in the volume was calculated by (V_2–V_1). The scaffolds impregnated in ethanol were removed from the cylinder, and the residual ethanol volume was recorded as V_3. The porosity of the scaffolds was obtained by the following equation

$$\text{Porosity}\,(\%) = \frac{(V_1 - V_3)}{(V_2 - V_3)} \text{x}\ 100 \qquad \text{---1}$$

In vitro enzymatic degradation

Nanofibrous scaffolds were exposed to collagenase enzyme (Sigma #C0773) to assess biological stability of the material and its degradation rate. A known weight of each sample in triplicate was taken and was air dried overnight at room temperature. All the samples were exposed with the collagenase enzyme (100 units/mL) for 24 h at 37°C (pH 7.4). After 24h, all the test samples were removed from the incubator, dried by blotting and left to air dry for 24 h at room temperature. Percentage of weight loss and final mass were calculated as simple ratio. Enzyme solutions were prepared in a phosphate buffer solution (PBS, pH7.4). The extent of biomaterial degradation was determined gravimetrically through weight loss.[26]

In vitro Swelling behavior

The *in vitro* swelling behavior of the nanofibrous scaffold were done by cutting the scaffold into a square piece (10 × 10 mm^2) and immersing it in PBS (pH7.4) at room temperature until the film reached swelling saturation. The weights of the scaffolds were measured after removing the surface wetness by using filter paper. The equilibrium-swelling ratio was calculated by using the following equation.

$$\text{Swelling}\,(\%) = \left(\frac{W_1 - W_0}{W_0}\right) \times 100 \qquad \text{---2}$$

where, W_0 and W_1 are the initial and the final weights of the film, respectively.[23]

In vitro drug release study

The drug release from the KCD-PG bilayered nanofibrous scaffold was determined by placing the KCD-PG nanofibrous in Franz-type diffusion cell at 37 ºC. The receiver compartment was filled with phosphate buffer solution (PBS, pH 7.4), which was stirred using a magnetic stirrer. At specific time intervals, 1 mL of buffer was removed from the receiver compartment and replaced with an equal quantity of phosphate buffer solution (PBS, pH 7.4) to maintain a constant volume. The drug content in the samples was determined by measuring the absorbance at 218 nm (Shimadzu UV 1800Ver. 2.43).[29]

The percentage of drug released from the KCD-PG nanofibrous scaffold was determined using the following equation.

$$A = \frac{Q_p}{Q_t} X 100 \qquad \text{---3}$$

where, A is the percentage of drug release from KCD-PG, Q_p is the quantity of drug release and Q_t is the total quantity of D loaded in the biosheet.[30]

In vitro Biocompatibility, Cell adhesion and proliferation studies

The Ethylene oxide sterilized scaffolds were further evaluated for the *in vitro* cell viability using MTT assay. The NIH 3T3fibroblast and human keratinocytes (HaCaT) cell lines were grown on the scaffolds placed in 24 well plates (Corning, NY) and maintained in DMEM with 10 % fetal calf serum supplemented with penicillin (120 units/mL), streptomycin (75 mg/mL), gentamycin (160 mg/mL), and amphotericin B (3 mg/mL) at 37 °C at a density of 5×10^4 cells/mL and then incubated over a time interval for 1, 3 and 7^{th} day in a humidified atmosphere of 5 % CO_2. Cells cultured in blank wells were used as control. After 1, 3 and 7^{th} day the culture medium was replaced with a serum-free medium containing10 µL of

Journal of Materials Chemistry B Accepted Manuscript

This journal is © The Royal Society of Chemistry 20xx

3-(4,5-dimethylthiazol-2-yl)-2,5-diphenyltetrazoliumbromide (MTT) and incubated at 37 °C for 4 h in a humidified atmosphere of 5 % CO_2. The medium was aspirated and then 500 µL/well of dimethylsulfoxide (DMSO) was added to dissolve the formazan needles with slow agitation for 10 min to yield a bluish purple solution. The absorbance of the dissolved solution was measured at 570 nm using Universal Microplate Reader.[26] The cell viability was calculated using following equation

$$\text{Cell viability (\%)} = \frac{OD_T}{OD_C} \text{x} 100 \qquad \text{---4}$$

Where OD_T is the absorbance of the cells in the presence of the nanofiber scaffold and OD_C is the absorbance of the control group (Incubated with culture media without scaffolds)

The cell attachment and proliferation of both NIH 3T3 and HaCaT cell lines were quantified for live cell and cell nuclei staining assay at regular time intervals (6, 24, 72 and 168 h), the medium was removed and the cells were fixed with 4 % Paraformaldehyde and washed with PBS for several times. Furthermore, each cell was first stained with DAPI solution (1.0 mg/ mL) for 15 min at 37 °C, and then washed again with PBS several times. Then Calcein AM solution (2 µM; 400 µL) was added and incubated for 30 min at 37 °C, Then the plates with scaffold were washed with PBS for several times and viewed at fluorescence microscope (EVOS FLoid Cell Imaging Station, Thermo fisher SCIENTIFIC, USA).[31] The Calcein AM associated live cell to produced green fluorescence, while DAPI associated with cell nuclei to produced blue fluorescence.

Antimicrobial activity

In this study, two bacterial strains were used, including one Gram positive bacteria *Staphylococcus aureus* (ATCC 11632) and one Gram negative bacteria *Escherichia coli* (ATCC 10536). All bacterial cultures were sub cultured and maintained aseptically. The antimicrobial activity of the KC-PG and KCD-PG bilayered scaffolds in square shape with 12 x12 mm were evaluated using modified disc diffusion method. About 100 µL [10^5 CFU (colony forming units)] of each bacterial culture was spread on the agar surface (Muller-Hinton agars) using a sterile glass spreader and the respective materials were placed. Then, the plates were incubated for 24 h at 37 ºC. The antibacterial activity was evaluated by measuring the zone of inhibition against the test organism.[32, 33]

In vivo studies

Male albino Wistar rats, weighing 180-200 g and 4-6 week of age, were used in this study. The rats were divided into five groups containing three animals in each group (control, KC, PG, KC-PG and KCD-PG scaffolds). The rats were acclimatized for a week prior to the commencement of the experiments. The housed rats were individually housed in 12 h light/dark cycle at 25 ± 1°C and were provided with standard rodent feed procured from M/s Hindustan Level Ltd. Feeds, Mumbai, India with water ad libitum.

Surgical procedure and dressing

Under aseptic condition the dorsal surface of the rat below the cervical region was shaved on its back after the intraperitoneal injection of standard anesthesia thiopentone sodium (dose 50 mg/kg body weight). A full thickness excision wound measuring 2 X 2 cm^2 were created. A square shaped silicone splint was placed, so that the wound is centered within the splint. The splint was fixed to the skin by suturing the corners to stabilize the position. Control (Group 1), wounds were dressed with sterile cotton gauze. Group 2 animals were dressed with KC scaffold, group 3 animals were dressed with PG nanofibrous scaffold, group 4 animals were dressed with KC-PG bilayered nanofibrous scaffold and group 5 animals were dressed with drug loaded KCD-PG bilayered nanofibrous scaffold. In both KC-PG and KCD-PG bilayerd nanofibrous scaffold PG side act as the wound contact layer at the wound site. The dressings were changed periodically at an interval of 5 days with the respective scaffolds for control, KC, PG, KC-PG and KCD-PG treated groups. The wounds were cleaned with sterile distilled water before dressing. Granulation tissues were collected on each of the five groups on 5^{th}, 10^{th}, and 15^{th} day post wounding and were stored at -80°C until analysis. The progress of wound healing in rats was evaluated by periodical monitoring of wound contraction, biochemical and histological analyses.

Planimetry: Rate of contraction and period of reepithelialization

The visual proof of the wound healing pattern was recorded from a constant distance by taking a digital photograph at an indicated time point. The period for full reepithelialization was calculated as the number of days required for the wounds to heal completely without a raw wound left behind the rats. The wound biopsies were noted, the rate of contraction and the surface area was measured by the standard palnimetric method, by tracing the wound on the transparent graph sheet. The percentage of wound contraction was measured using the formula:

$$\text{Wound contraction (\%)} = \frac{\text{wound area day 0} - \text{wound area day(n)}}{\text{wound area day 0}} \text{X} 100 - 5$$

where n = number of days (5^{th} , 10^{th} , 15^{th} and 18^{th} day). The results were analyzed by one-way ANOVA at 5 % error. The tensile strength of the healed wound tissues were measured at the end of the experiments.[33]

Journal of Materials Chemistry B Accepted Manuscript

Tensile strength measurements of the wound tissues

The untreated and treated wound tissues collected at the end of the experiments were analyzed for its tensile strength. The healed wound tissues were removed after the sacrification of rats from each group at end of the day 18. The harvested tissues were trimmed into strips 20 mm long and 2 mm wide, with the area of original wound lying lengthwise in the centre of the sample. Mechanical properties such as tensile strength (MPa) and percentage of elongation at break (%) were measured using a universal testing machine (Instron model 4501).

Biochemical analyses of the excision wounds

The excised tissues were biochemically analyzed to estimate the total amount of collagen (hydroxylproline) content in defatted granulation tissue by the method of Woessner[34], hexosamine was estimated by the method of Elson and Morgan[35], Uronic acid was measured by the method of Schiller et al.[36], and Protein content was analyzed using Lowery et al [37], for both treated and untreated wound tissues.

Histopathology study of granulation tissue

The periodically collected granulation tissues from the wound sites along with healthy skin of 2 mm surrounding the wound on 5th, 10th and 15th day of post wound creation were used for histopathology. The 10 % buffered formalin fixed samples were dehydrated by a graded alcohol series, cleared in xylene and embedded in paraffin blocks. The 4 µm thick sections of the samples were sliced and stained with both haematoxylin-Eosin and Masson's trichrome stain (Fisher Scientific). The stained sections were examined using a microscope and photomicrographed (TCM400, Labomed).

Real time PCR (RT-PCR)

The regenerated skin was collected on 5th, 10th and 15th day of the post wound creation with all visible fat and healthy skin was trimmed for isolating the total RNA using Total RNA extraction kit (iNtRON Biotechnology, South korea) according to the instruction given by the manufacturer. One microgram of total RNA was used to reverse transcriped using power cDNA synthesis kit (iNtRON Biotechnology, South korea). The PCR reaction was performed in the thermal cycler (Applied Biosystems Step One^{TM} Real-Time PCR System, Foster City CA) using the following conditions: Amplification was followed by 5 minutes at 95 °C, and 40 cycles of 15 seconds at 94 °C, 1 minute at 60 °C, with final extension for5 minutes at 72 °C min to extend any incomplete single strands.[38] Primer sequences were designed using Primer-BLAST (http://www.ncbi.nlm.nih.gov/tools/primer-blast/) and were synthesized. All the primer pairs were analyzed by Primer-BLAST to ensure specificity for the intended target gene within the human genome. VEGF, forward 5′-A GAGTGGGAGGGAAGCTCTTAG-3′, reverse 5′-CGGGATTTCTTGCGCTTTCG-3′ (511); EGF, forward 5′ TGGAAAAGATGGCTGCCACTGGGTC-3′ reverse 5′ GTGTTCCTCTAGGACCACAAACCA-3′ (430); and TGF-β, forward 5′-CACACAGTCCGCTACTTCGT-3′ reverse 5′-CGGG TGCTGTTGTAAAGTGC-3 (434).

Statistical analysis

Results are presented as mean ± S.D. (n = 3). ANOVA (analysis of variance) and student's t-test were done to determine the significant differences among the groups. The observed differences were statistically significant when $p< 0.05$. All statistical analyses were performed using GraphPad Prism software.

Results and Discussion

Characterization

Scanning electron microscope (SEM)

The SEM micrograph of bilayered nanofibrous scaffolds and individual scaffolds revealed the uniform smooth nanofibrous morphology with beadles nature were depicted in the **Fig.1.**

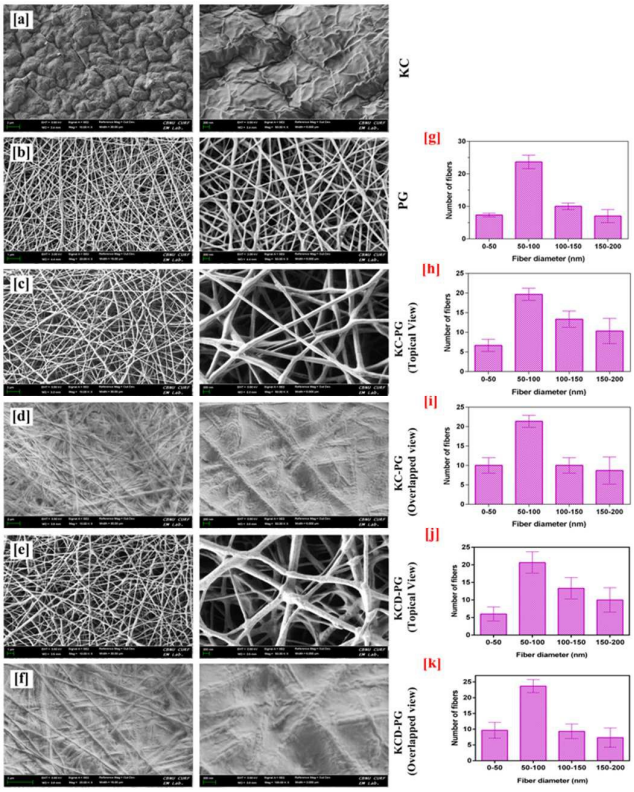

Figure 1 (a-f) SEM micrograph (a) KC, (b) PG, (c) KC-PG (Topical view), (d) KC-PG (Overlapped view), (e) KCD-PG (Topical view) and (f) KCD-PG (Overlapped view) scaffolds with their respective fiber diameter (g-k)

Journal of Materials Chemistry B Accepted Manuscript

This journal is © The Royal Society of Chemistry 20xx

Please do not adjust margins

Polyhydoxybutyric acid (P) is a hydrophobic polymer while gelatin (G) is hydrophilic in nature. A common solvent system for both polymers ensures maximum interaction between the two. [39] Hence, 1,1,1,3,3,3 hexafluroisopropanol was used for this purpose. hydrophilic gelatin with its cell binding motifs will aid in initial adhesion of the cells, while P will attract the keratinocytes which prefer a more hydrophobic surface. The ECM mimicking structure will further ensure an enhanced adhesion when compared to solution cast sheets of KC.

The KC, PG and KC-PG scaffold were obtained to have a uniform pore size and distribution. The bilayered nanofibrous scaffold possesses to have high surface to volume ratio that supports in easy cell adhesion and attachment. The SEM morphology of the bilayered nanofibrous matrix scaffold was depicted in two ways as primary layer (KC-bottom view) secondary layer (PG-topical view) and both intermediate merged layer (both KC and PG overlapped surface). In addition, cross-sectional image of the bilayered nanofibrous scaffold was depicted in **Fig.2**. It is observed that only KC scaffold showed a more delicate structure. However, the fabrication of bilayered scaffold of KC and PG showed a highly increased and better property when compared with the individual KC and PG scaffold. Overall the bilayered scaffold has tends to have fibrous and smoothed structure in a single scaffold that aids in cell adhesion and faster wound healing.[26] The diameter of the PG, KC-PG (topical view) and KC-PG (overlapped view) exhibited to have 72±15 nm, 78±25 nm and 86±28 nm respectively. In addition more than 60 % of the nanofiber has the diameter in the range of 50-100 nm. The size of the individual PG nanofiber scaffold was correlated with the bilayered nanofibrous KC-PG scaffold at the interface to have increased diameter. The conductivity of the PG nanofiber over the semi solid nature of the KC during electrospinning play a major role in increases the diameter of the nanofiber at the interface. However fiber diameter retains more or less equal when more fibers were electrospun over the KC-PG scaffold interface.[40]

Fourier Transform Infrared Spectra (FTIR)

To investigate the chemical composition and conformational changes of the bilayered nanofibrous matrix scaffold after electrospinning were confirmed using FTIR spectroscopy **(Fig.3)**. All the corresponding peaks of the D, KC, PG, KC-PG and KCD-PG were found in the IR spectrum with no solvent peak noticed during the electrospinning process. The spectrum of KC and KC-PG exhibited the characteristic peaks of amide I and II bands were observed at 3300– 3400 cm^{-1} and 1550–1650 cm^{-1} of keratin with strong absorption band at 2600–3300 cm^{-1} and 1142 cm^{-1}corresponds OH and polysaccharide structure in chitosan. However, after electrospinning of KC-PG and KCD-PG scaffolds showed peaks of poly (3-hydroxybutric acid) in the range 1720-1740 cm^{-1} (ester carbonyl group) and 1270-1280 cm^{-1} (CH group) with gelatin presents its two amide I (1600-1660 cm^{-1}), amide II (~1550 cm^{-1}) absorption bands. In addition, PG exhibited at exhibit absorption bands at 2933 cm^{-1} corresponds to the Ch_2 and Ch_3 with gradual broad band due to the overlapping of N-H and O-H stretching vibrations (3300–3600 cm^{-1}) correspond to gelatin. The KCD-PG scaffolds showed an overlapping peaks at 1398, 1656 and 1059 cm^{-1} revealing the interaction between drug and polymer.[39, 40]

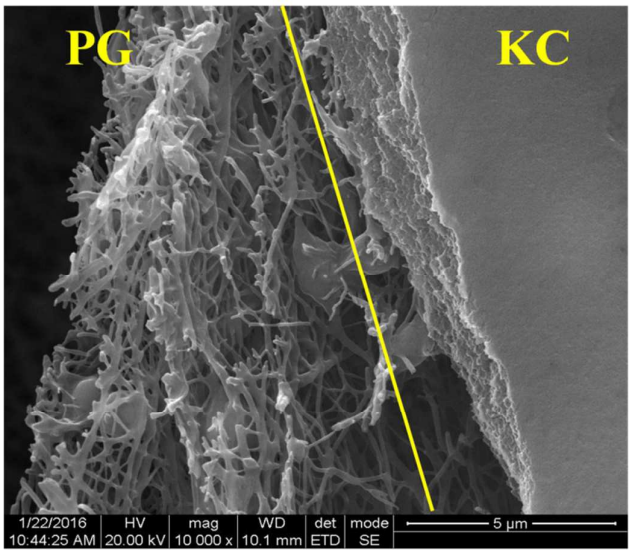

Figure 2 Cross-sectional SEM micrograph of bilayered KC-PG scaffolds

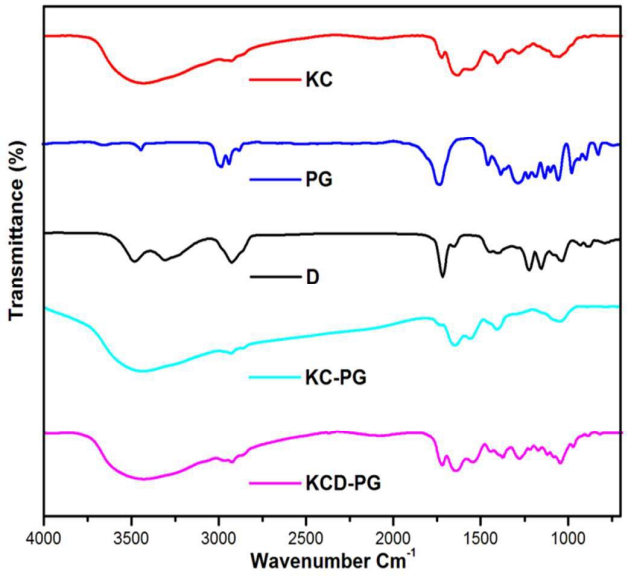

Figure 3 FTIR spectra of the scaffolds

Journal of Materials Chemistry B Accepted Manuscript

X-ray photoelectron spectroscopy

X-ray photoelectron spectroscopy (XPS) wide spectra scan was exhibited in **Fig. 4**. The spectra indicated that both KC and KC-PG scaffold shows the carbon, oxygen, nitrogen and sulphur peaks as expected. The nitrogen and sulphur were the characteristic element of keratin present in both the scaffolds. However, the electrospun PG nanofibrous over the KC scaffold partially mask the presence of sulphur peak with decrease in the binding energy with S1s peak. The corresponding nitrogen (N1s) peaks in both scaffolds appears. The carbon has binding energies with 284. 9 eV to 288.2eV and oxygen 1s has binding energy with 532.1 eV to 533.2 eV correspond s to the amine, amide and peptides. The nitrogen 1s and sulphur 1s core level spectrum with binding energy of peak at 400.eV and 153.6 eV respectively corresponds to the amide and sulphide. Moreover, the presence of sulphide aids in formation of S=S of the disulphide bond in fibrous protein keratin makes the bilayered nanofibrous scaffold more rigid with high mechanical property.[34, 43]

Tensile strength

The mechanical property of the bilayered KC-PG and KCD-PG nanofibrous scaffolds were investigated from the tensile strength and the elongation at break (Table S1). The KC-PG and KCD-PG nanofibrous scaffold were flexible with a tensile strength of 25.49±1.06and 24.82±0.57 MPa respectively. It is reported in our previous paper that KC exhibited moderated tensile strength when compared to PG scaffold with 21.14 and 14.56 MPa respectively.[23, 38] It was noticed that bilayered nanofibrous scaffold showed a significantly enhanced tensile strength. Since the KC scaffold presumably forms as a backbone for the PG scaffold to act as double layered scaffold to exhibit increase in tensile strength in KC-PG scaffold. However, the flexibility and soft matrix of the nanofibrous scaffold was most prominent for its use in behavior and sterilization during the process application onto the wound surface. KCD-PG scaffold showed slight decrease in the tensile strength due to the presence of drug within the KC scaffold.[26]

In vitro swelling behavior

The swelling ability of the bilayered nanofibrous scaffold material is important property for the evaluation of the wound dressing. The swelling ability of the KC, PG and KC-PG scaffolds were given in the Fig. S1. The swelling ratio of the KC, PG and KC-PG dressing material exhibited significantly higher swelling ability when compared to that of the normal single layered KC and PG scaffold material. The swelling of the scaffold was important to keep the wound dry by absorbing the wound exudates. The KC biosheet layer acquires more efficiency in absorbing more exudates and the PG aids

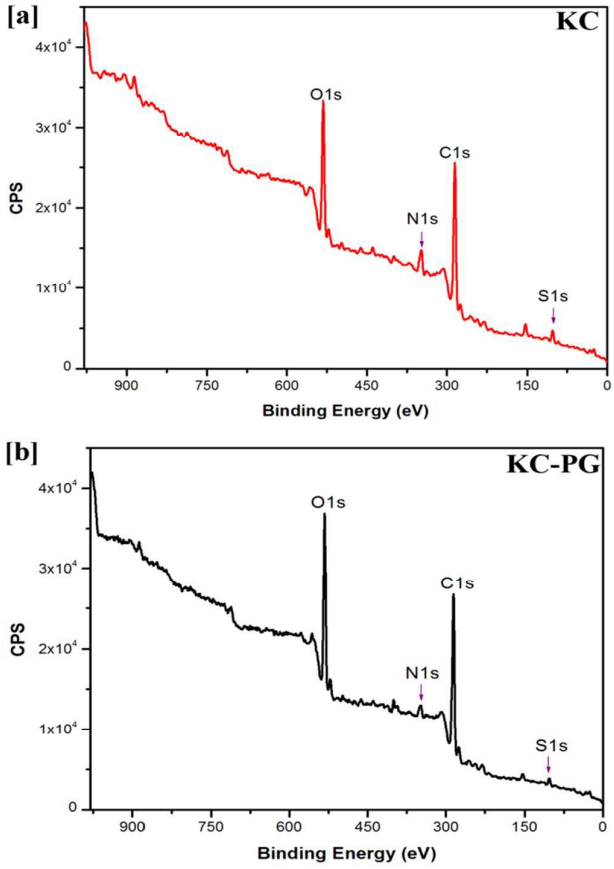

Figure 4 XPS full spectra of the (a) KC and (b) KC-PG scaffold

in the cell adhesion proliferation with the support of the nanofibrous matrix. The higher water adsorption ability of the bilayered nanofibrous matrix attributes to the increased porosity; thereby having the potency to absorb more exudates and keeps wound surface with oxygen permeability.[44]

Porosity

The porosity of the nanofibrous scaffold was an important factor for easy tissue formation which aid in delivering the essential protein and growth factors to the cell recognition site for the proliferation of the fibroblast cells. The porosity of the scaffolds was exhibited in the Fig S2. The porosity of the KC, PG, KC-PG and KCD-PG scaffolds with liquid displacement method was found to be 65.97 %, 75.95 %, 73.27 % and 73.70 % respectively. The individual PG nanofibrous scaffold showed a higher porosity when compared to the other scaffolds. The KC and PG porosity (73.70 %) observed in the present study reveals that this could be used as an efficient bilayered scaffold for tissue engineering application. The porous and soft nature of the nanofibrous scaffold should attain maximum porosity not only to accomplish the oxygen and nutrient exchange but also maintain cellular infiltration. Generally the cellular infiltration

Journal of Materials Chemistry B Accepted Manuscript

 This journal is © The Royal Society of Chemistry 20xx

Please do not adjust margins

should be within the range of 60 to 90 %. In the current work the porosity was calculated to be above the range of 72 %, which is more sufficient for cell infiltration from the nanofibrous scaffold.[45]

In vitro enzymatic degradation

The nanofibrous scaffold has to possess a controlled biodegradation to attain a suitable biomaterial in tissue engineering application. The weight losses of the nanofibrous scaffold due to collagenase activity were exhibited in the Fig. S3. The KC and PG scaffold exhibited 65.67 % and 73.28 % of weight loss respectively compared to that of the KC-PG and KCD-PG nanofibrous scaffold. Moreover, the weight loss of the scaffold is directly corresponds to the amount of weight loss attained by the scaffold with respect to that of enzyme. The *in vitro* enzymatic activities of all the scaffolds were assessed to configure a more biological stability against the collagenase enzyme. The enzymatic biodegradation of the KC-PG nanofibrous scaffold was enhanced as compared with that of the KC and PG scaffolds. The KC-PG and KCD-PG showed no significant difference in the weight loss when compared to that of the individual KC and PG scaffold. Nevertheless, the major weight loss attained was probably due to the degradation of the chitosan in KC scaffold and gelatin in PG nanofibrous scaffold. The hydrophobic nature of the PHB and keratin mostly forms as the backbone for the increased stability of the nanofibrous scaffold.[46]

In vitro drug release study

In order to deliver a more sustainable controlled delivery of drug through bilayered scaffold (Fig. S4). Herein, the KC soft matrix scaffold loaded D over that PG nanofibrous scaffold were used to meet the desired timeframe in the physiological environment on the wounded surface. The *in vitro* drug release from the bilayered scaffold showed an initial burst release of 20.4 % was measured at 1 h in phosphate buffer solution (pH 7.4) at 37°C from D loaded biocompatible KCD-PG nanofibrous scaffolds. The initial burst release from the KCD-PG scaffold was due to the loosely bounded surface drug over the soft matrix KC scaffold. In addition, the drug release from the soft KC matrix is triggered by the controlled swelling and biodegradation of the nanofibrous scaffold. Moreover, the KCD-PG nanofibrous scaffold showed a sustained drug release 77 % over a period of 78h with enhanced absorption of exudates, which significantly facilitates the prevention of infection at the wound site.[29, 47]

Though electrospun scaffolds have been demonstrated to elute drug at the wound site after implantation, the mechnical and physiochemical properties of the scaffolds are greatly altered due to the addition of the drug. Hence, KC films with drug mupirocin was used the base material over which the electrospun fibers were coated. The KC films ensured an increased mechanical strength and controlled drug release, while the PG electrospun layer ensured an enhanced cell adhesion and proliferation.

In vitro Biocompatibility, Cell adhesion and proliferation studies

The *in vitro* biocompatibility of the bilayered nanofibrous scaffold is found to be necessary for the wound dressing material. The *in vitro* biocompatibility of the bilayered nanofibrous KCD-PG scaffolds was evaluated towards NIH 3T3 and HaCaT cell lines after 1, 3, and 7 days by MTT assay (Fig. S5 and S6). In the bilayered nanofibrous scaffold the PG side was seeded with cells and exhibited with high cell viability in both cells. However, the nanofibrous morphology of PG aids in high cell adhesion and proliferation for enhanced synthesis of collagen and fast wound healing activity.

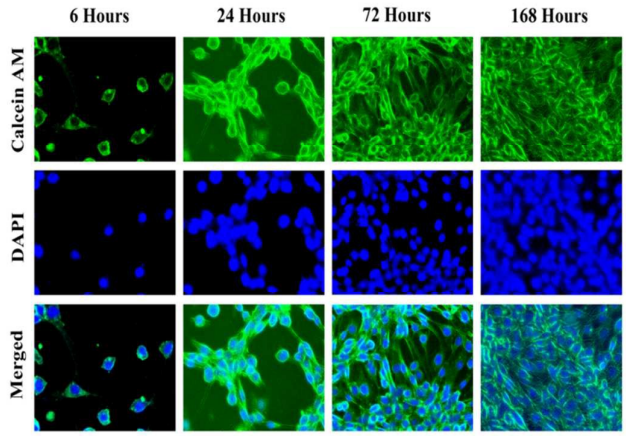

Figure 5 Calcein AM - DAPI fluorescence staining images of NIH 3T3 fibroblast cell adherence and proliferation onto the KCD-PG bilayered nanofibrous scaffold at various time intervals of 6, 24, 72 and 168 h. The scale bar measures in 100 µm

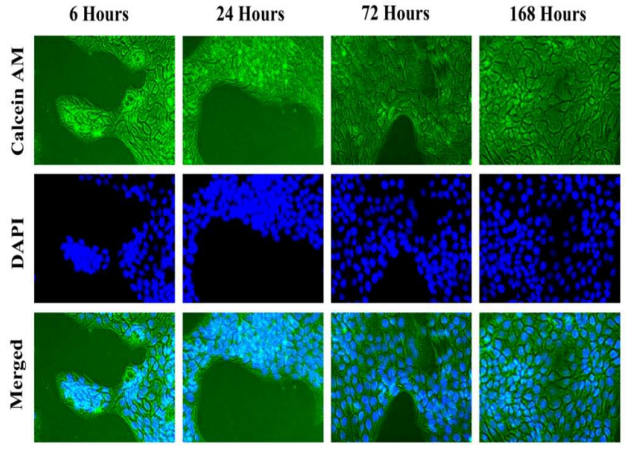

Figure 6 Calcein AM - DAPI fluorescence staining images of the Human (HaCaT) keratinocytes cell adherence and proliferation onto the KCD-PG bilayered nanofibrous scaffold at various time intervals of 6, 24, 72 and 168 h. The scale bar measures in 100 µm

Journal of Materials Chemistry B Accepted Manuscript

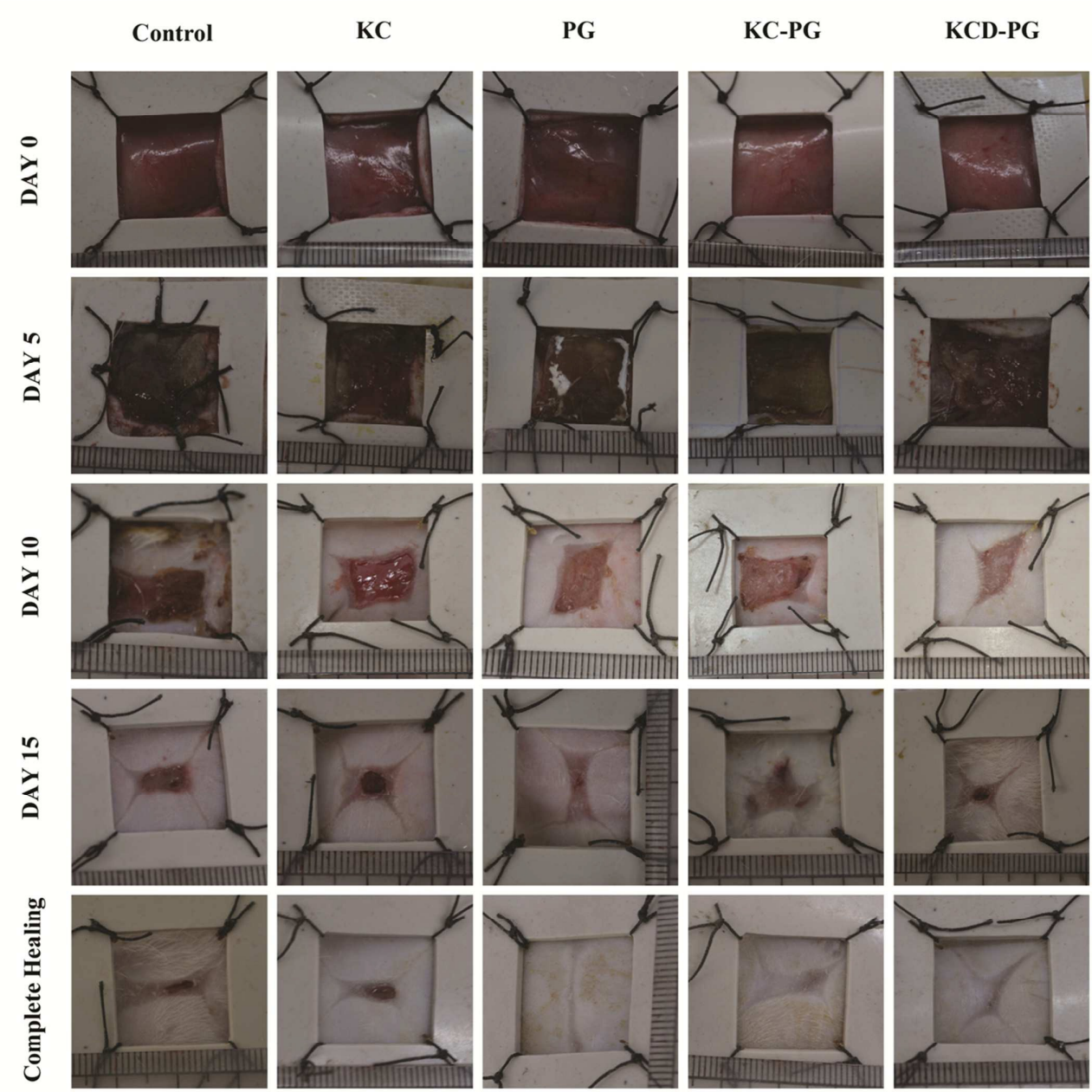

Figure 7 Photographic images showing healing pattern of excisional wounds taken from same distance on different days.

The cell viability of the scaffold showed increased cell numbers. In the KCD-PG bilayered scaffold, PG scaffold was found to be better cell seeding surface. Since the nanofibrous scaffold act as the base for the cell adhesion, easy cell proliferation and cell attachment. Besides that, KCD-PG nanofibrous scaffold exhibited significantly higher cell proliferation with high cell numbers at day 7. Furthermore, the presence of keratin in the bilayered scaffold assists in creating cell binding motifs (RGD (Arg-Gly-Asp), LDV (Leu-Asp-Val)) for the easy cell adhesion, proliferation and cell attachment.[23]

The nanofibrous surface morphology of the KCD-PG nanofibrous scaffold influences the certain cell-material interface for the effective material biocompatibility with NIH 3T3 and HaCaT cell lines. The cell morphology with the cell adhesion was assessed through fluorescent staining of Calcein AM and DAPI staining as shown in **Fig. 5 and 6**. The KCD-PG nanofibrous scaffold showed through wide spread of cells. Moreover, nanofiber matrix and cells forms the

Journal of Materials Chemistry B Accepted Manuscript

Please do not adjust margins

intercalated structure within the nanofiber surface pertained to have better cell adhesion and attachment. The PG nanofibrous scaffold act as the anchored material for both NIH 3T3 and HaCaT cell lines to exhibit with high cell numbers with better cell proliferation.

Comparable to our previous study with KC soft matrix scaffold with horn keratin the bilayered nanofibrous scaffold-cast film finds uniform spreading of both cells on the KC-PG scaffold.[23] The keratin in the bilayered nanofiber matrix enhances to provide a substrate for production of the ECM with specific interaction through the cell binding motifs for good attachment of cells.[48] The merge of cell over the scaffolds suggest the formation of rich ECM on the scaffolds, indicating the high amount of proliferation of cells.[46]

Antimicrobial activity

The efficient dressing material should possess a strong antimicrobial property to prevent the growth of bacterial infection. Fig. S7 shows the antimicrobial property of the bilayered nanofibrous scaffold against *S. aureus* and *E. coli*. The KCD-PG scaffold shows excellent inhibitory activity with both the organisms. However, KC-PG nanofibrous scaffold did not showed any zone of inhibition. The gradual release of antibiotic mupirocin exhibited bactericidal activity against both gram positive and gram negative bacterium. Nevertheless, KCD-PG nanofibrous scaffold showed a clear zone of inhibition.[32, 49]

In vivo study

Photographic evaluation and planimetric studies

Although photographic evaluation and planimetric analysis were carried out for all animals, only one representative from each group is shown in **Fig. 7**. During the Photographic evaluation it was observed that PG exhibited faster healing than KC scaffold. However, the KCD-PG bilayered nanofibrous scaffold was fabricated with drug to substantiate the antimicrobial property to the KC scaffold. Moreover, the PG side supports the cell growth and proliferation with simultaneous absorption of exudates to the KC sides, which keeps the wound free from infection for enhanced healing. The visual evidence of *in vivo* wound healing was done by taking photograph using NIKON D5100 DSLR camera from a fixed distance for all experimental animals and the planimetric experiments were performed periodically. The results exhibited to indicate faster healing in the experimental group 5 treated with KCD-PG, when compared to the other groups.[50]

Rate of wound contracture and period of re-epithelialization

The wound assessment plays a major role in predicts the rate of shriveling of the epithelium of the excisional wounds, that was calculated from the planimetric sheet photographs using Image J software program from the wound tracing sheet. One- way ANOVA were performed and exhibited to have a statistical significance between the groups and all the groups reveals significantly different on the precised day. Rate of wound contraction in all groups were shown in the **Fig. 11 (a)**. The complete closing of wounds was observed with slow rate of contraction in control group treated with cotton gauze than the experimental groups at various time intervals. The group treated with KC and PG showed a moderate wound healing when compared with the KC-PG and KCD-PG group. The significant increase in the percentage of wound contraction was observed in PG than the KC comparatively in all days. The bilayered KC-PG and drug loaded KCD-PG material possess to have consistent and faster healing rate on all days, when compared to that of the other treated groups. However the KCD-PG treated group exhibits superior healing over the other treated groups. In addition, the healing rate of group 5 was significantly better than group 4. The electrospun nanofibrous membrane with KC as a bilayered scaffold treated groups exhibits rapid wound contraction from the day 12 when compared to that of the control. The control and KC treated groups observed to have wound closing at 19^{th} and 18^{th} day respectively. The PG, KC-PG and KCD-PG treated groups showed a similar amount of wound contraction with complete closure was observed on the 17^{th}, 18^{th} and 16^{th} day respectively. The difference between the groups treated with KC, PG and KC-PG showed with significant difference ($P< 0.05$) from 10^{th} day only, whereas group treated with KCD-PG exhibits a significantly improved rate of contraction from the 8^{th} day. Nevertheless, the constant increase in wound closure with complete healing with KC-PG and KCD-PG group was observed on the 18^{th} and 17^{th} day respectively whereas , KC, PG treated groups exhibited to have complete wound closure at 19^{th} day and 18^{th} day respectively, control group has taken almost 21 days for complete healing. Overall the wound contraction and planimetric results associated well with the photographic wound evaluated pattern.[33, 51, 52]

Biochemical analyses of the excision wounds

The total collagen, hexosamine, and uronic acid content in the granulation tissues of the control and the treated experimental groups of the rats on specified days of scarification after wound creation were shown in **Fig. 8**. The granulation tissue was found to have accumulated with predominant extracellular protein in wounds with

Journal of Materials Chemistry B Accepted Manuscript

Please do not adjust margins

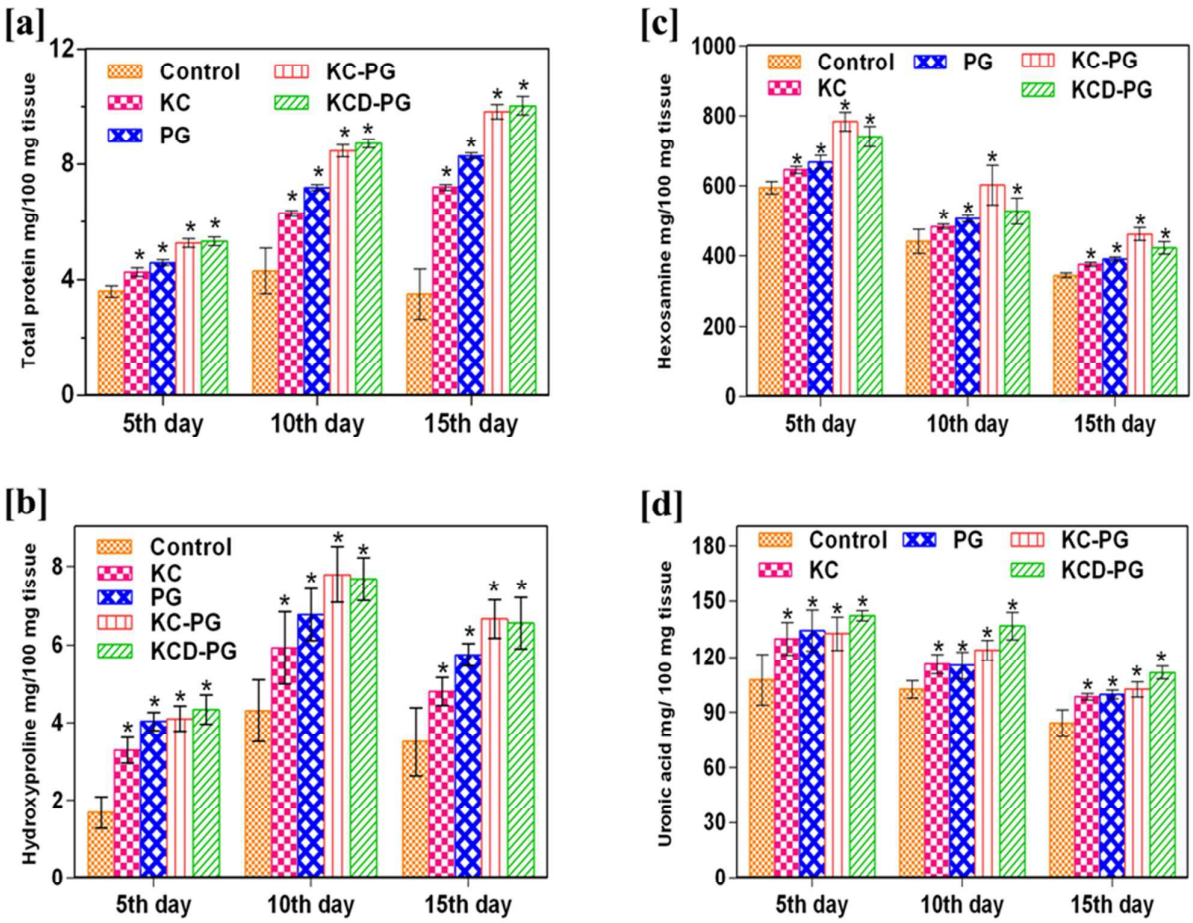

Figure 8 Levels of biochemical contents in the granulation tissue for control and experimental animal groups on 5th, 10th and 15th day; (a) total protein, (b) hydroxyproline, (c) hexosamine and (d) uronic acid. Values are expressed as mean ± SD and the level of significance is expressed as * corresponding to $p < 0.05$ respectively compared with the corresponding control group.

major role of collagen deposition by the intiation of fibroblast migration towards the healing of wound with increased haemostasis, cell-cell interaction, cell-matrix interaction and reepithelialization.[53] Assessment of collagen from the granulation tissue was found to have hydroxyproline as the major constituent.[54] The collagen content was found to have increased level in control and treated groups up to 10th day with significant difference among the groups that has 27, 35, 44 and 43 % high amount of collagen in KC, PG, KC-PG and KCD-PG treated groups respectively when compared to the control group. However 15th day exhibits significantly decrease in the collagen content due to the stabilized level of collagen. The effective healing of the wound by the improved fibroblast cell attachment toward the reepithelialization of skin by increased collagen synthesis with high collagen content all over the wound healing phases but in control group found to have decreased collagen synthesis throughout the healing phase.[55]

The collagen content of wound samples plays the pivotal role in production of ECM followed by the moderate increase in the hexosamine content. The increasing level of collagen and protein suppress the production of hexosamine. However the increase in the level of hexosamine was observed when the collagen content decreases in all treated groups when compared with control.

The KC-PG treated group that exhibited to have increase level of hexosamine content throughout the experiment. All treated groups observed to have significantly higher level of hexosamine content when compared with the control. The KCD-PG treated group signifies a marginal decrease in the hexosamine level from the day 5 to day 15 when compared with the KC-PG treated group. Since the decrease in the hexosamine content in the entire treated group and the control groups correspondingly signifies the increase in collagen content level in all experimental groups.[56]

Similar marginal decreasing trend has been observed in the uronic acid content in all treated groups and the control from the day 5 to

Journal of Materials Chemistry B Accepted Manuscript

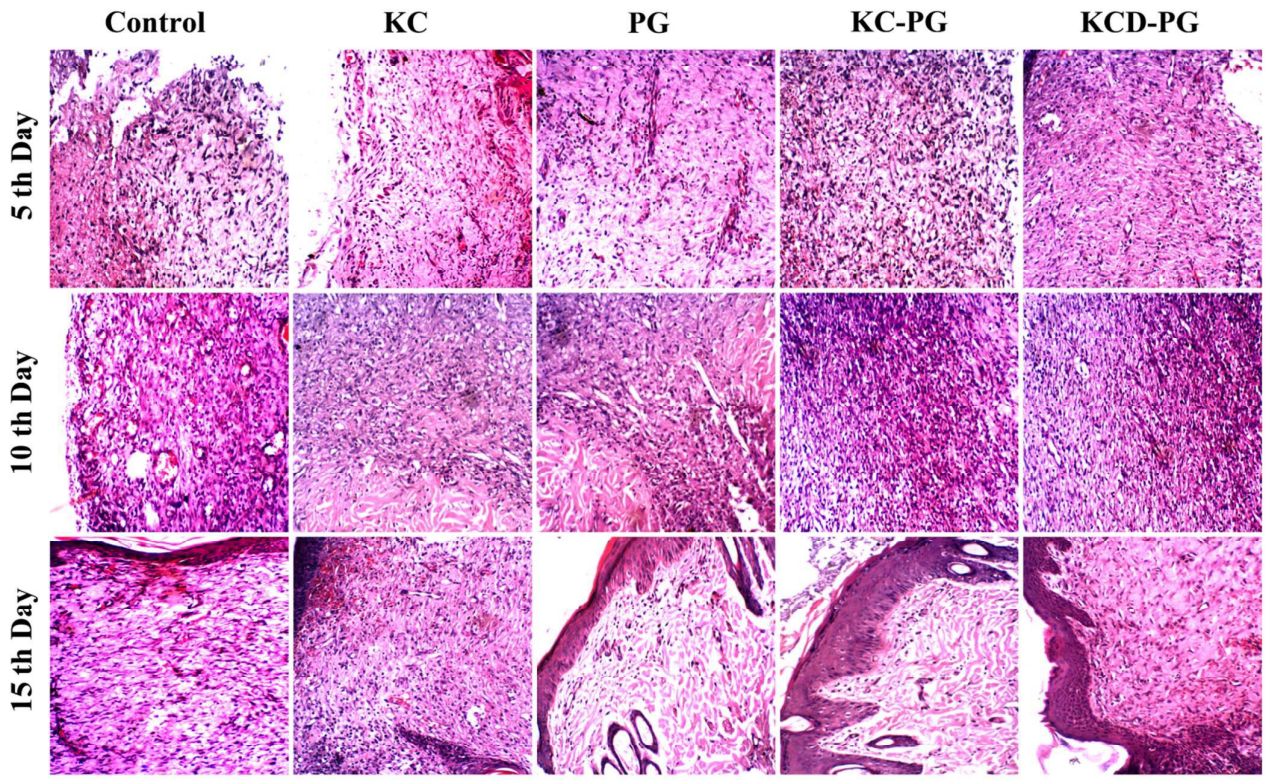

Figure 9 Haematoxylin and eosin staining of control and treated groups on 5th, 10th and 15th day after wound creation. (Magnification: 40×)

day 15. Consistently the group treated with KCD-PG found to have significant increase in the uronic acid content level throughout the experiment. Nevertheless the presence of nanofibrous matrix (PG) with KC membrane as a double layer has contributed to have enhanced collagen synthesis with effective healing by mimicking the function of ECM for faster healing at the wound site.[57]

Tensile strength of the healed wound

The tensile strength of the excised wound tissue of the KC, PG, KC-PG and KCD-PG treated group and control group has been exhibited in Fig. S8. The KC-PG and KCD-PG treated group showed increased in tensile strength than other treated group and control. Due to the increase in collagen production during the initial stages in wound healing, imparts with 2.2 fold increase in tensile strength, which is statistically significant when compared to the control group. Since after the deposition of collagen during the maturation phase, it founds clear in restoration of collagen in the healed wounds to obtain increase tensile strength.[57] However, the KC-PG and KCD-PG treated group showed significant increase in strength than the other treated groups. The increased collagen synthesis during the proliferative phase at 5th and 10th day after wounding has tends to exhibits increase in tensile strength in healed skin tissues with the formation of collagen fibers during the post wounding during the maturation phase.[38, 33]

Histological observation

The wounded tissues were performed with histological examination for the treated and control groups using h and E and Masson trichrome staining has been shown in **Fig. 9 and 10**. The photomicrographs of histological sections using h and E staining exhibited to have the epithelium, connective tissue, fibroblast proliferation, new blood capillaries and collagen deposition. The treated group shows less number of inflammatory cells and high number of fibroblast when compared to that of the control group. The day 5stained tissue section of all treated group showed increase in deposition of collagen with blood capillaries and inflammatory cells when compared to the control. The more inflammatory cells on the day 10 of the stained tissues section in the clearly indicates that the KC-PG and KCD-PG bilayered treated group with increased healing process which significantly accelerate wound healing with enhanced collagen deposition on the other hand when compared with the other treated and control group. However, KC, PG treated group showed epithelium and connective tissues with collagen deposition they showed moderate healing compared to that of the KC-PG and KCD-PG treated group and control. The day 15 of the stained tissue

Journal of Materials Chemistry B Accepted Manuscript

Please do not adjust margins

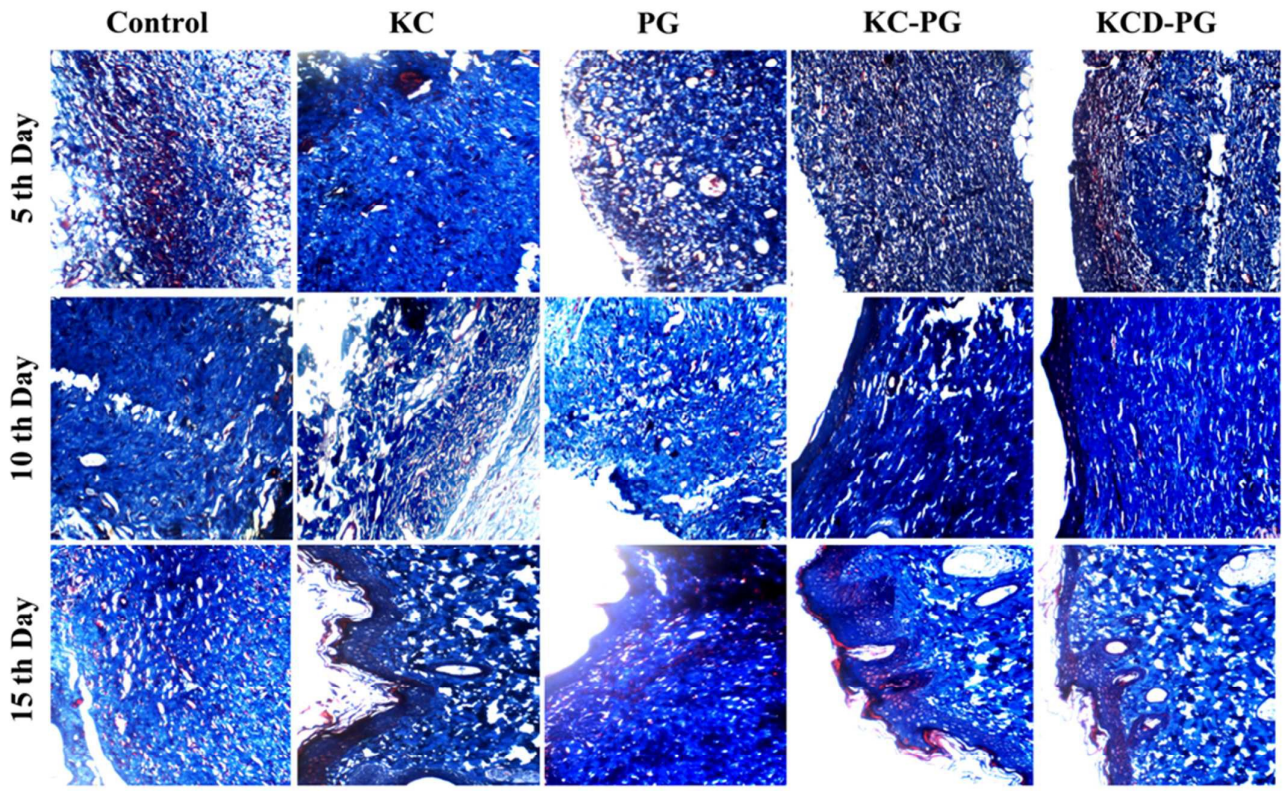

Figure 10 Masson trichorme staining on control and treated group on 5th, 10th and 15th day after wound creation. (Magnification: 40×)

section clearly indicates the reasonable epithelial cell formation with complete healing in bilayered treated groups. Moreover the KC and PG treated group's forms a moderate healing than control. The reduced inflammatory cells during the day 5, 10 and 15 clearly indicate the faster healing than control group. The presence of keratin and the nanofibrous matrix in the bilayer group was well established with good tissue repair and remodeling. Nevertheless, control group showed inconsistent healing with slow epithelialization and less collagen deposition. Ultimately, the KCD-PG treated group exhibited as an effective nanofibrous matrix for scar less wound healing.[58, 59]

The Masson trichrome staining results clearly states the bilayer KC-PG and KCD-PG group helps in collagen remodeling and degradation with enhanced collagen formation which affords high tensile strength and reduces the scar formation. This in turn brings the fibroblast proliferation by enhanced neovascularization for the early phase of wound healing by the stimulating the synthesis of glycosaminoglycan, proteoglycans and collagen. The treated groups showed an augmented healing rate when compared to control. The drug in the KCD-PG treated group avoids the bacterial infection during the promotion of fibroblast and formation of extracellular matrix with better healing. This clearly indicates that the KCD-PG nanofibrous matrix can be used as an alternative biomaterial in wound dressing application.[33, 60]

Expression of VEGF, EGF and TGF β in response to wound dressing material in wound healing

The expression of the growth factors with various complex signaling factors involves in the wound closure. The expression of main growth factors such as EGF, VEGF and TGF-β in response to different dressing material used in this study is shown in **Fig 11 (b-d)**. β actin was used as a control in this study. The wound healing is the interplay of variety of cells, cytokines and growth factor as regulator to healing process. The KC and PG material treated groups on 5th, 10th and 15th day showed similar expression levels compared to that of the control. KC-PG and KCD-PG expressed statistically high expression on day 10 in EGF, VEGF and TGF-β respectively than control. However, the expression level reduced significantly in both KC-PG and KCD-PG treated group on day 15.

The EGF enhance the fibroblast activation and act as a leading edge of dermal-epidermal junction by promoting granulation tissue formation during wound healing from the initial days .[61, 9] The EGF showed a significant increase in expression level from 5th to10th day, in all treated group when compared to the control. Whereas, KCD-PG treated groups showed statistically significant increase in day 10

Journal of Materials Chemistry B Accepted Manuscript

Please do not adjust margins

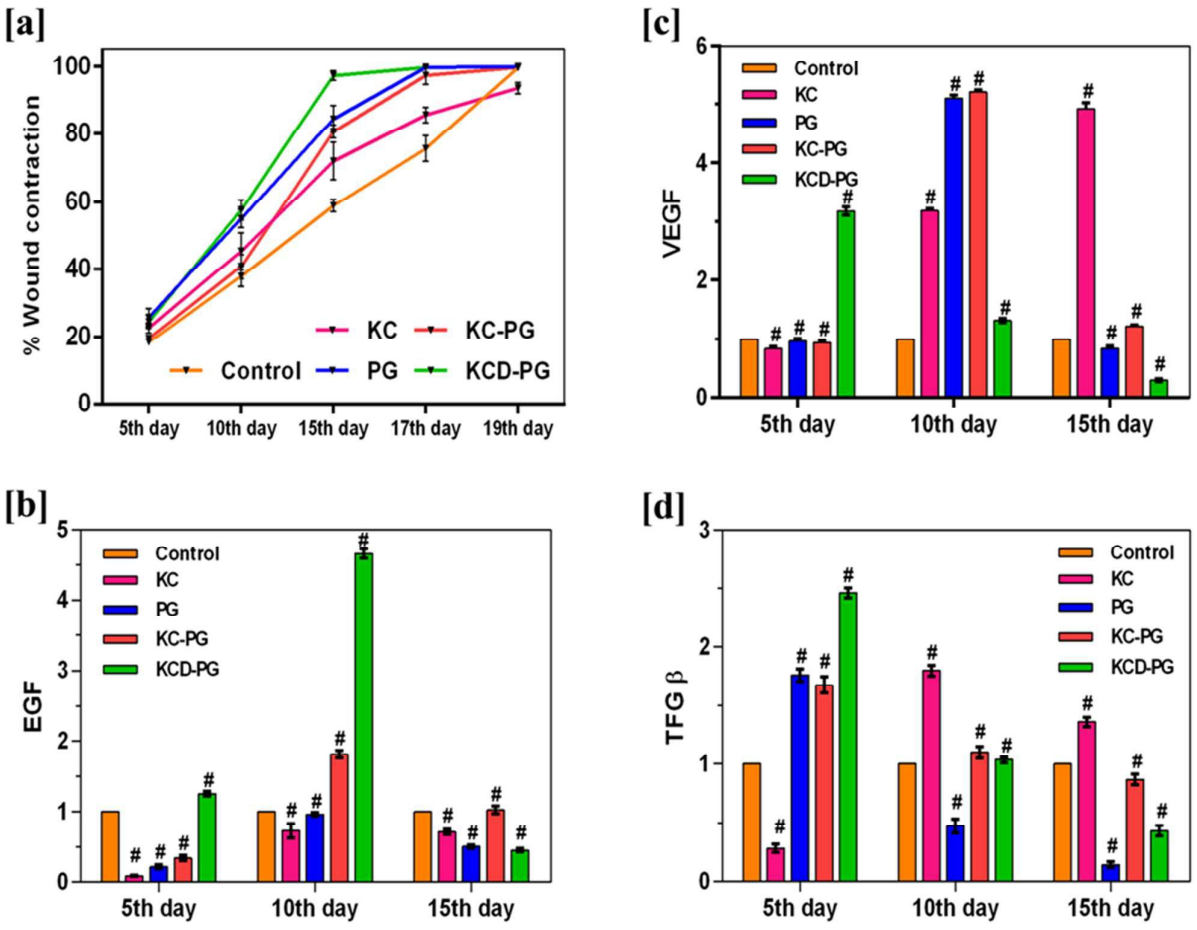

Figure 11 (a) Percentage wound contraction, RT-PCR analysis of mRNA expression profiles for the (b) EGF, (c) VEGF and (d) TGF-β, (n = 3) results are presented as mean ± SD; statistically significant data are given as # P < 0.05

than KC-PG treated groups. The high and moderate expression on day 15 in KCD-PG treated groups facilitates with rapid wound healing process.

The expression level of TGF-β was significantly high in all treated groups at day 5 and exhibited a constant decreasing level up to 15th day. Whereas, TGF-β initiate the formation of granulation tissue and matrix modulation for the genes expressed with ECM formation including fibronectin and collagen.[62] The researchers describe that lowering TGF-β level at day 15 reduce scar formation and increases the rate of wound healing due to the support of fibroblast and keratinocytes.[64 - 66]

All the dressing material showed a homologous expression level of VEGF during the day 5 and day 15. However, there was a significant increase in expression level of KC treated group at day 15. The mRNA expression level of all scaffold treated groups was normal when compared to that of the day 10. The initial decrease in the expression level after wound creation followed by the significant increase tends to produce primary cells during the 15th day.[66] The KC, PG and KC-PG treated group showed rise in expression level of VEGF during the day 10, which is the key factor in multiple events of wound healing by stimulating angiogenesis, epithelialization and collagen deposition by producing smooth muscle cells, platelets, keratinocytes, macrophages, neutrophils and endothelial cells.[67, 68] The decrease in the expression level of EGF, VEGF and TGF-β in the day 15 reveals the increase in wound healing. However, the suppression of growth factor level at day 15 inversely corresponds to the significant healing of wounds. The healing with significant reduction in the respective growth factor plays a important role in healing of wound with the migration, proliferation, production of fibroblast, keratinocytes, neutrophils, macrophages and endothelial cells over a period of time thereby helping faster healing.[69]

Conclusion

To summarize the present study, a bilayered nanofibrous with high porosity and swelling was fabricated through electrospinning by

Journal of Materials Chemistry B Accepted Manuscript

Please do not adjust margins

loading mupirocin into the dual matrix layered wound dressing material using silicone splint model. In this case the physiochemical property such as morphology, degradability and mechanical analysis were improved with bilayered nanofibrous scaffold. The cell-material interaction with the bilayered nanofibrous scaffold revealed enhanced biocompatibility, cell adhesion and proliferation with both cell lines. The bilayered nanofibrous scaffolds shown to augment the process of excision wound healing by increasing the migration of fibroblast, collagen synthesis during granulation tissue formation with enhanced expression of growth factor during the remodeling phase of the wound healing by preventing infection at the wound site. Thus, bilayered nanofibrous KCD-PG scaffold act as a prominent wound dressing for excision wound based on the biocompatibility and wound healing efficacy.

Author Contributions

The manuscript was written through contributions of all authors. All authors have given approval to the final version of the manuscript.

Notes

The authors declare no competing financial interest.

Acknowledgments

The author SS thanks UGC, New Delhi for financial support (RGNF Fellowship [F1-17.1/2012-13/RGNF-2012-2013-SC-TAM-21595 / (SA-III/Website]). The author RGP thanks the Council of Scientific and Industrial Research (CSIR) (India grant no. 31/6(395)/2014-EMR-I), New Delhi, India, for providing the funds to carry out this study.

Reference

1. Murugan, R, Ramakrishna, S, *Tissue Eng,* 2006, **12**, 435.
2. Tan hong Bo, Wang Fu You, Ding Wei, Zhang Ying, Ding G Jing, Cai Di Xin, Yu Kai Fu, Yang Jun, Yang Liu, Xu Yong Qing, *Biomed Environ Sci,* 2015, **28**, 178-189.
3. Jin Soo Lim, Gyeol Yoo. Effects of Adipose-derived Stromal Cells and of their Extract on Wound healing in a Mouse Model*J Korean Med Sci*2010, **25**, 746-51.
4. Frank, S, hubner, G, Breier, G, Longaker, M. T, Greenhalgh, D. G, Werner, S*, J. Biol. Chem*1995, **270**, 12607-12613.
5. Carpenter, G, Cohen, S, *Annu. Rev. Biochem,* 1979, **48**, 193-216.
6. Assoian, R. K, Grotendorst, G. R, Miller, D. M, Sporn, M. B, *Nature*1971, **309**, 804–806
7. Rheinwald, G, Green, H, *Nature*1977, **265**, 421-424.
8. Do Gi Pyun, hyun Jun Choi, hyoung Soon Yoon, Thavasyappan Thambi, Doo Sung Lee, *Colloids Surf B Biointerfaces,* 2015, **135**, 699-706.
9. Gregory, S. Schultz, Annette, Wysocki. Interactions Between Extracellular Matrix And Growth Factors In Wound healing*Wound Rep Reg,* 2009, **17**, 153–162 .
10. Mo, X. M, Xu, C. M. , Kotaki, M, Ramakrishn, S*,* 2004, **25**, 1883–1890.
11. Naveen, Nagiah, Giriprasath, Ramanathan, Liji, Shobana, Sivakumar, Singaravelu, Tiruchirapalli, Sivagnanam Uma, Tirupattur, Srinivasan Natarajan, *Journal of Biomaterials and Tissue Engineering,* 2013, **3**, 1–6.
12. Linhao, Li, Yuna, Qian, Chongwen, Lin, haibin, Li, Chao, Jiang, Yonggang, Lv, Wanqian, Liu, Kaiyong, Cai, Olive,r Germershaus, Li Yang, *J. Mater. Chem, B*2015, **3**, 859.
13. Aluigi, A, Zoccola, M, Vineis, C, Tonin, C, Ferrero F, Canetti M. Study On The Structure And Properties Of Wool Keratin Regenerated From Formic Acid *Int J Biol Macromol*2007, **41**, 266–73.
14. Rouse, J. G, Van, Dyke M. E. A Review of Keratin-Based Biomaterials for Biomedical Applications*Materials (Basel)*2010, **3**, 999–1014.
15. Duan, B, Yuan, X, Zhu, Y, Zhang, Y, Li, X, Zhang, Y, Yao, K. A, *Euro Polym Jnl*2006, **42**, 2013-2022.
16. Ma, L, Gao, C, Mao, Z, Zhou, J, Shen, J, hu, X, han, C*,* 2003, **24**, 4833-4841.
17. Piras, A. M, Chiellini, F, Chiellini, E, Nikkola, L, Ashammakhi, N, *J Bioact Compatible Polym 2008,* **23**, 423–443
18. Lee, S. Y, *Biotechnol Bioeng 1996,* **49**, 1–14.
19. Williamson, D. H, Mellanby, J, Krebs, H. A, *Biochem J 1962,* **82**, 90–96.
20. Barbetta, A, Dentini, M, Vecchis, M. S. D, Filippini, P, Formisano. G, Caiazza, S, *Adv. Funct. Mater*2005, **15**, 118.
21. Dai, T, huang, Y, Sharma, S. K, hashmi, J. T, Kurup, D. B, hamblin, M. R, *Recent Pat. Anti-Cancer Drug Discov,* 2010, **5**, 124–151.
22. Seza, Ozge Gonen, Melek, Erol Taygun, Sadriye Ku cukbayrak, *Chemical Engineering Technology*, 2015, **38**, 844-50.
23. Singaravelu, S, Ramanathan, G, Raja, M. D, Sagar, Barge, Uma, T. S, *Materials letters,* 2015, **152**, 90-93.
24. Chuan-Ling Zhang, Shu-hong Yu, Chem *Soc. Rev,* 2014, **43**, 4423.
25. Giriprasath, Ramanathan, Sivakumar, Singaravelu, Raja, M. D, Uma, Tiruchirapalli Sivagnanam, *Micron,* 2015, **78**, 28–32.
26. Giriprasath, Ramanathan, Sivakumar, Singaravelu, Raja, M. D, Naveen, Nagiah, Padmapriya, P, Ruban, K, Krishnasamy, Kaveri, Natarajan, T. S, Uma, Tiruchirapalli Sivagnanam,

Journal of Materials Chemistry B Accepted Manuscript

This journal is © The Royal Society of Chemistry 20xx

Paramasivan, Thirumalai Perumal, *RSC Adv,* 2016, **6**.DOI: 10.1039/C5RA19529B.

27. Naveen, Nagiah, Lakshmi, Madhavi, Anitha, R, Anandan, C, Natarajan, Tirupattur Srinivasan, Uma Tirichurapalli Sivagnanam, *Materials Science and Engineering, C*2013, **33**, 4444–4452.
28. Naveen, Nagiah, Lakshmi, Madhavi, Anitha, R, Anandan, C, Natarajan, Tirupattur Srinivasan, Uma Tirichurapalli, Sivagnanam, *Polym. Bull*2013, **70**, 2337–2358.
29. Nagiah, N, Ramanathan. G, Sobhana, L, Sivagnanam, U. T, Srinivasan, N. T, *International Journal of Polymeric Materials and Polymeric Biomaterials,* 2014, **63**, 583–585
30. Yin, X. C, Li, F. Y, he, Y. F, Wang, Y, Wang, R. M, *Biomater. Sci,* 2013, **1**, 528–536.
31. hoJun, Jeon, Geunhyung, Kim, *J. Mater. Chem. B*2014, **2**, 171.
32. Rui, Zhao, Xiang, Li, Bolun, Sun, Yan, Tong, Ziqiao, Jiang, Ce, Wang, *RSC Adv,* 2015, **5**, 16940.
33. Thangavelu, Muthukumar, Kannan Anbarasu, Dharmalingam, Prakash, Thotapalli, Parvathaleswara Sastry, *Colloids and Surfaces B: Biointerfaces 2014,* **121**, 178–188.
34. Woessner, Jr. The Determination Of hydroxyproline In Tissue And Protein Samples Containing Small Proportions Of This Imino Acid *J. Arch Biochem Biophys,* 1961, **93**, 440- 447.
35. Elson, L. A, Morgan, W. T. A. Colorimetric Method For The Determination Of Glucosamine And Chondrosamine J. *Biochem J,* 1933, **27**, 1824-1828.
36. Schiller, S, Slover, G. A, Dorfman, A, *J Biol Chem,* 1961, **236**, 983-987.
37. Lowry, O. h, Rosebrough, N. J, Farr, A. L, Randall, R. J, *J Biol Chem,* 1951, **193**, 265-275.
38. Thangavelu, Muthukumar, Dharmalingam, Prakash, Kannan, Anbarasu, Baskar, Santhosh Kumar, Thotapalli, Parvathaleswara Sastry, *RSC Adv,* 2014, **4**, 64267.
39. Naveen Nagiah, Richard Johnson, Roy Anderson, Winston Elliott, and Wei Tan, Langmuir, 2015, **31**, 12993–13002.
40. Tao, Liu, Xinbo, Ding, Dongzhi, Lai, Yongwei, Chen, Ridong, Zhang, Jianyong, Chen, Xinxing, Feng, Xiaoyi, Chen, Xianyan, Yang, Ruibo, Zhao, Kai, Chend, Xiangdong, Kong, *J. Mater. Chem. B*2014, **2**, 6293.
41. Zivanovic, S, Li, J, Davidson, P. M, Kit, K ,*Biomacromolecules,* 2007, **8**, 1505–10.
42. Jotiram, K. P, Prasad, R. G. S. V, Jakka, V. S, Aparna, R. S. L, Phan,i A. R, *Nano BiomedEng,* 2012; 4, 144-149.
43. Jiashen, Li,Yi Li, Lin, Li, Arthur, F.T. Mak, Frank, Ko, Ling, Qin, *Polymer Degradation and Stability, 2009,* **94**, 1800–1807.
44. Mi, F.L, Shyu, S.S, Wu Y.B, Lee, S.T, Shyong, J.Y, huang, R.N, *Biomaterials,* 2001, **22**, 165–173.
45. Jelena Rnjak-Kovacina, Steven, G. Wise , Zhe, Li, Peter, K.M. Maitz, Cara, J. Young, Yiwei, Wang, Anthony, S. Weiss, *Biomaterials,* 2011, **32**, 6729-6736.
46. Narendra K. Singh, Sunil K. Singh, Debabrata Dash, Biswa Pratim Das Purkayastha, Jagat K. Roy, Pralay Maiti, *Mater. Chem,* 2012, **22**, 17853.
47. YoungWon, Koo, hyeongjin, Lee, Suji, Kim, No-Joon Song, Jin-Mo Ku, Jaehwan Lee, Chang, hyun Choi, Kye Won Park, Geunhyung, Kim, *RSC Adv* 2015, **5**, 44943.
48. Paulina, Sierpinski, Jeffrey, Garrett, Jianjun, M, Peter, Apel, David, Klorig, Thomas, Smith, Andrew Koman, L, Anthony Atala, Mark Van Dyke, *Biomaterials* 2008*,* **29**, 118–128.
49. Runze, Wang, Zheng, Wang, Song, Lin, Cheng, Deng, Fan, Li, Zhijian, Chen, hua, he, *RSC Adv,* 2015, **5**, 40141.
50. Kumar, P. T. S, Lakshmanan, V. K, Anilkumar, T. V; Ramya, C, Reshmi, P, Unnikrishnan, A. G, Nair, S. V; Jayakumar, R, *ACS Appl. Mater. Interfaces,* 2012, **4**, 2618–2629.
51. Ragothaman, Murali, Thangavel, Ponrasu, Kalirajan, Cheirmadurai, Palanisamy, Thanikaivelan, *Journal of Biomedical Materials Research Part A*, 2016, **104**, 388–396.
52. He, Xu, Fang, Lv, Yali, Zhang, Zheng, fangYi, Qinfei, Ke, Chengtie,Wu, Mingyao Liu, Jiang, Chang. *Nanoscale,* 2015, 7, 18446-18452.
53. Raghow, R. The Role of Extracellular Matrix In Postinflammatory Wound healing And Fibrosis*FASEB J*1994, **8**, 823–831.
54. Chithra, P, Sajithlal, G. B, Chandrakasan, G. Influence Of Alovera On The Glycosaminoglycans In The Matrix Of healing Dermal Wounds In Rats *J. Ethanopharmacol,* 1998, **59**, 179–186.
55. Pilcher, B. K, Sudbeck, B. D, Dumin, J. A, Welgus, h. G, Parks, W. C, *Arch. Dermatol. Res,* 1998**, 209**, 37–46
56. Noorjahan, S. E, Sastry, T. P, *J. Biomed. Mater. Res. B: Appl. Biomater*2004, **71**, 305–312.
57. Young, Ju. Lee, ho Sung, Son, Gyeong, Bok Jung, Ji hye Kim, Samjin Choi, Gi-Ja Lee, hun-Kuk, Park, *Materials Science and Engineering C*2015, **51**, 43–50.
58. Yuyu, Qiu, Liying, Qiu, Jing, Cui, Qufu, Wei, *Materials Science and Engineering C*2016, **59**, 303–309.

Journal of Materials Chemistry B Accepted Manuscript

59. Jiantao, Lin, Caihong, Li, Yi, Zhao, Jianchan, hu, Li-Ming, Zhang, *ACS Appl. Mater. Interfaces*2012, **4**, 1050−1057.
60. Deepachitra, R, Ramnath, V, Sastry, T. P. Graphene Oxide, *RSC Adv,* 2014, **4**, 62717-62727
61. Thomas, W. Lawrence, Robert, F. Diegelmann, *Clinics in Dermatology*1994, **12**, 157-16.
62. Greenwel, P, Inagaki, Y, hu, W, Walsh, M, Ramirez, F, *J Biol Chem*1997, **272**, 19738–45.
63. Lee, h. S, Kooshesh F, Saude,r D. N, Kondo, S. Modulation of Tgf-Beta 1 Production From human Keratinocytes By Uvb *Exp Dermatol*., 1997, **6**, 105–10.
64. Eppley, B. L, Woodell, J. E, Higgins, *J. Plast Reconstr Surg,* 2004, **114**, 1502–8.
65. Rolfe, K J, Richardson, J, Vigor, C, Irvine, L. M, Grobbelaar, AO, Linge, C, *J Invest Dermatol,* 2007, **127**, 656–67.
66. Jazwa, A, Loboda, A, Golda, S, Cisowski, J, Szelag, M, Zagorska, A, Sroczynska, P, Drukala, J, Jozkowicz, A, Dulak, *J. Free Radic Biol Med,* 2006, **40**, 1250–63.
67. Nissen, N. N, Polverini, P. J, Koch, A. E, Volin, M. V, Gamelli, R. L, DiPietro, L. A., *Am J Pathol,* 1998, **152**, 1445–52.
68. Gaudry M, Bregerie O, Andrieu, V, El, Benna. J, Pocidalo, M. A, hakim J, Neutrophils *Blood*, 1997, **90**, 4153–61.
69. Neil, T, Bennett, M. D, Gregory, S. Schultz, Gainesville, Florida, *Am J Surg,* 1993, **165**, 729 –737.

Journal of Materials Chemistry B Accepted Manuscript

This journal is © The Royal Society of Chemistry 20xx

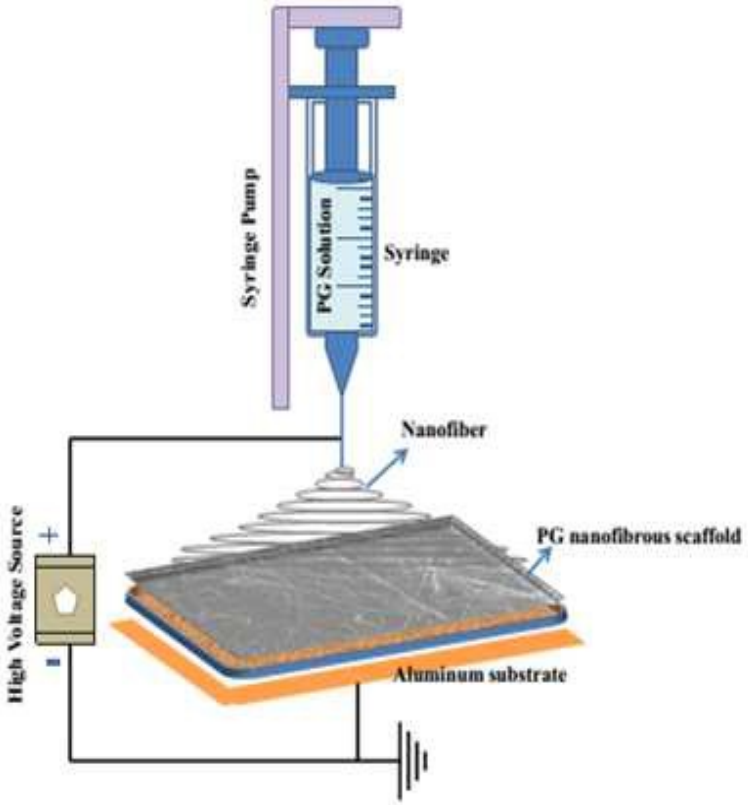

The fabricated bilayered nanofibrous scaffold found to be simple and also easily up scalable technique due to its high surface to volume ratio. The nanofibrous scaffold mimics the function of the extra cellular matrix with enhanced *in vitro* biocompatibility and *in vivo* wound closure.

Journal of Materials Chemistry B Accepted Manuscript